Hindawi
Journal of Function Spaces
Volume 2021, Article ID 5580687, 10 pages
https://doi.org/10.1155/2021/5580687

Research Article

Solving the Modified Regularized Long Wave Equations via Higher Degree B-Spline Algorithm

Pshtiwan Othman Mohammed,[1] **Manar A. Alqudah**,[2] **Y. S. Hamed**,[3] **Artion Kashuri**,[4] **and Khadijah M. Abualnaja**[3]

[1] *Department of Mathematics, College of Education, University of Sulaimani, Sulaimani, Kurdistan Region, Iraq*
[2] *Department of Mathematical Sciences, Faculty of Sciences, Princess Nourah Bint Abdulrahman University, P.O.Box 84428, Riyadh 11671, Saudi Arabia*
[3] *Department of Mathematics and Statistics, College of Science, Taif University, P. O. Box 11099, Taif 21944, Saudi Arabia*
[4] *Department of Mathematics, Faculty of Technical Science, University Ismail Qemali, Vlora, Albania*

Correspondence should be addressed to Pshtiwan Othman Mohammed; pshtiwansangawi@gmail.com and Manar A. Alqudah; manarqudah@yahoo.com

Received 24 January 2021; Revised 16 February 2021; Accepted 19 February 2021; Published 3 March 2021

Academic Editor: Giovany Malcher Figueiredo

The current article considers the sextic B-spline collocation methods (SBCM1 and SBCM2) to approximate the solution of the modified regularized long wave (MRLW) equation. In view of this, we will study the solitary wave motion and interaction of higher (two and three) solitary waves. Also, the modified Maxwellian initial condition into solitary waves is studied. Moreover, the stability analysis of the methods has been discussed, and these will be unconditionally stable. Moreover, we have calculated the numerical conserved laws and error norms $\mathscr{L}_2$ and $\mathscr{L}_\infty$ to demonstrate the efficiency and accuracy of the method. The numerical examples are presented to illustrate the applications of the methods and to compare the computed results with the other methods. The results show that our proposed methods are more accurate than the other methods.

1. Introduction

The regularized long wave (RLW) equation is defined by the following nonlinear partial differential equation [1]:

$$\sigma_\tau + \sigma_\eta + \zeta\sigma\sigma_\eta - \mu\sigma_{\eta\eta\tau} = 0, \tag{1}$$

where μ and ζ are positive parameters. This equation was first introduced by Peregrine [1] and after that by Benjamin et al. [2] to describe the behavior of the undular bore. It has also a great role in physics science, especially in physics media since it is useful in describing a phenomenon in different disciplines, such as the nonlinear transverse waves in magneto hydrodynamics waves in plasma, ion-acoustic waves in plasma, shallow water, longitudinal dispersive waves in elastic rods, phonon packets in nonlinear crystals, and pressure waves in liquids gas bubbles.

There are many analytical methods to obtain the solution of the RLW equation for certain boundary and initial conditions; for example, see [2, 3]. Also, the numerical solutions of the RLW equation has been studied by many researchers via various methods, such as finite difference methods [4, 5], Fourier pseudospectral methods [6], various models of finite element methods including least square, collocation, and Galerkin methods [7–9], mesh-free method [10], and Galerkin finite element methods [11–13].

The generalized form of the RLW equation is known as the GMRLW equation which is given by

$$\sigma_\tau + \sigma_\eta + \zeta\sigma^p\sigma_\eta - \mu\sigma_{\eta\eta\tau} = 0, \tag{2}$$

where p is a positive parameter. In the extension of nonlinear dispersive waves, this equation has an important role. There are many numerical methods to investigate its solution. For more details, we advise the reader to visit [14–17]. In the current attempt, we consider a special case of the GMRLW (namely, the MRLW) equation, given by

$$\sigma_\tau + \sigma_\eta + \zeta\sigma^2\sigma_\eta - \mu\sigma_{\eta\eta\tau} = 0, \quad (3)$$

subject to the boundary conditions ($B.Cs$):

$$\begin{aligned} \sigma(\rho_1, \tau) &= \beta_1, \quad \sigma(\rho_2, \tau) = \beta_2, \\ \sigma_\eta(\rho_1, \tau) &= 0, \quad \sigma_\eta(\rho_2, \tau) = 0, \\ \sigma_{\eta\eta}(\rho_1, \tau) &= 0, \quad \sigma_{\eta\eta}(\rho_2, \tau) = 0, \end{aligned} \quad (4)$$

and the initial condition ($I.C.$) is taken as

$$\sigma(\eta, 0) = f(\eta), \quad (5)$$

where $f(\eta)$ is assumed to be localized disturbance inside the given interval. There are many authors who obtained the numerical solution of the MRLW equation; for example, Gardner et al. [18] used the cubic B-spline finite element method, Prenter [19] used variational and spline methods, and Khalifa et al. [20] used finite difference method; in [21], they used the Adomian decomposition method, they also in [22] used the collocation method, and Fazal-i-Haq et al. [23] used the quartic B-Spline collocation method to get an approximate solution of the MRLW equation.

In this study, inspired by the abovementioned studies, we use the sextic B-spline collocation methods to approximate the solution of the MRLW equations (3)–(5). The rest of the paper is organized as follows. In Sections 2.1 and 2.2, we discuss the B-spline collocation methods I and II and their stability analysis on the proposed MRLW equation. Section 3 is dedicated to the numerical implementations and comparison of our obtained results with those obtained in the literature: Section 3.1 is for single solitary wave, and Sections 3.2 and 3.3 are for interactions of multiple solitary waves. A conclusion is subsequently given in Section 3.

2. The Methods of B-Spline Collocation

Let us partition the finite interval $[\rho_1, \rho_2]$ into a uniform mesh by points η_ℓ, $\ell = -3, -2, \cdots, \mathrm{J}+2$ such a way that $\rho_1 = \eta_0 < \eta_1 < \cdots < \eta_{\mathrm{J}-1} < \eta_\mathrm{J} = \rho_2$, where $\Delta\eta = \mathrm{y} = \rho_2 - \rho_1/\mathrm{J} = \eta_\ell - \eta_{\ell-1}$. Then, we state the sextic B-spline collocation methods I (SBCM1) and II (SBCM2).

2.1. The SBCM1. We know that the sextic B-splines are usually defined on $\mathrm{J}+1$ nodes over a given interval $[\rho_1, \rho_2]$ with 12 additional nodes outside the interval $[\rho_1, \rho_2]$. The additional nodes may be given as follows:

$$\begin{aligned} &\eta_{-6} < \eta_{-5} < \eta_{-4} < \eta_{-3} < \eta_{-2} < \eta_{-1} < \eta_0, \\ &\eta_\mathrm{J} < \eta_{\mathrm{J}+1} < \eta_{\mathrm{J}+2} < \eta_{\mathrm{J}+3} < \eta_{\mathrm{J}+4} < \eta_{\mathrm{J}+5} < \eta_{\mathrm{J}+6}. \end{aligned} \quad (6)$$

The sextic B-splines B_ℓ at the knots η_ℓ are defined as [1]

$$B_\ell(\eta) = \frac{1}{\hbar^6}\begin{cases} (\eta-\eta_{\ell-3})^6, & [\eta_{\ell-3}, \eta_{\ell-2}], \\ (\eta-\eta_{\ell-3})^6 - 7(\eta-\eta_{\ell-2})^6, & [\eta_{\ell-2}, \eta_{\ell-1}], \\ (\eta-\eta_{\ell-3})^6 - 7(\eta-\eta_{\ell-2})^6 & \\ +21(\eta-\eta_{\ell-1})^6, & [\eta_{\ell-1}, \eta_\ell], \\ (\eta-\eta_{\ell-3})^6 - 7(\eta-\eta_{\ell-2})^6 & \\ +21(\eta-\eta_{\ell-1})^6 - 35(\eta-\eta_\ell)^6, & [\eta_\ell, \eta_{\ell+1}], \\ (\eta-\eta_{\ell+4})^6 - 7(\eta-\eta_{\ell+3})^6 & \\ +21(\eta-\eta_{\ell+2})^6, & [\eta_{\ell+1}, \eta_{\ell+2}], \\ (\eta-\eta_{\ell+4})^6 - 7(\eta-\eta_{\ell+3})^6, & [\eta_{\ell+2}, \eta_{\ell+3}], \\ (\eta-\eta_{\ell+4})^6, & [\eta_{\ell+3}, \eta_{\ell+4}], \\ 0 & \text{otherwise}, \end{cases} \quad (7)$$

for $\ell = -3, -2, \cdots, \mathrm{J}+2$, and the set $\{B_{-3}, B_{-2}, \cdots, B_{\mathrm{J}+2}\}$ of sextic B-splines can be a basis over the interval $[\rho_1, \rho_2]$.

The approximate solution $\sigma_\mathrm{J}(\eta, \tau)$ of the GMRLW equation to the exact solution $\sigma(\eta, \tau)$ will be determined as follows:

$$\sigma_\mathrm{J}(\eta, \tau) = \sum_{\ell=-3}^{\mathrm{J}+2} \vartheta_\ell(\tau) B_\ell(\eta), \quad (8)$$

where the time dependent parameters $\vartheta_\ell(\tau)$ will be determined from the sextic B-spline collocation formula of equation (3).

In view of equation (8) and Table 1, the nodal values $\sigma^{(i)}$, $i = 0, 1, \cdots, 5$ at the knots η_ℓ can be found as

$$\begin{aligned} \sigma_\ell &= \vartheta_{\ell+2} + 57\vartheta_{\ell+1} + 302\vartheta_\ell + 302\vartheta_{\ell-1} + 57\vartheta_{\ell-2} + \vartheta_{\ell-3}, \\ \sigma'_\ell &= \frac{6}{\mathrm{y}}(\vartheta_{\ell+2} + 25\vartheta_{\ell+1} + 40\vartheta_\ell - 40\vartheta_{\ell-1} - 25\vartheta_{\ell-2} - \vartheta_{\ell-3}), \\ \sigma''_\ell &= \frac{30}{\mathrm{y}^2}(\vartheta_{\ell+2} + 9\vartheta_{\ell+1} - 10\vartheta_\ell - 10\vartheta_{\ell-1} + 9\vartheta_{\ell-2} + \vartheta_{\ell-3}), \\ \sigma_\ell^{(3)} &= \frac{120}{\mathrm{y}^3}(\vartheta_{\ell+2} + \vartheta_{\ell+1} - 8\vartheta_\ell + 8\vartheta_{\ell-1} - \vartheta_{\ell-2} - \vartheta_{\ell-3}), \\ \sigma_\ell^{(4)} &= \frac{360}{\mathrm{y}^4}(\vartheta_{\ell+2} - 3\vartheta_{\ell+1} + 2\vartheta_\ell - 2\vartheta_{\ell-1} + 3\vartheta_{\ell-2} - \vartheta_{\ell-3}), \\ \sigma_\ell^{(5)} &= \frac{720}{\mathrm{y}^5}(-\vartheta_{\ell+2} + 5\vartheta_{\ell+1} - 10\vartheta_\ell + 10\vartheta_{\ell-1} - 5\vartheta_{\ell-2} + \vartheta_{\ell-3}). \end{aligned} \quad (9)$$

Now, we implement the collocation method at the nodes η_i, $i = 0, 1, \cdots, \mathrm{J}$. Also, we substitute the nodal variables σ_ℓ and its derivatives at the knots η_i in equation (9) into equation

Table 1: The sextic B-spline values at the grid points.

η	$\eta_{\ell-3}$	$\eta_{\ell-2}$	$\eta_{\ell-1}$	η_{ℓ}	$\eta_{\ell+1}$	$\eta_{\ell+2}$
Q_ℓ	1	57	302	302	57	1
$\hbar Q'_\ell$	6	150	−240	−240	−150	−6
$\hbar^2 Q''_\ell$	30	270	−300	−300	270	30
$\hbar^3 Q_\ell^{(3)}$	120	120	−960	960	−120	−120
$\hbar^4 Q_\ell^{(4)}$	360	−1080	720	720	−1080	360
$\hbar^5 Q_\ell^{(5)}$	720	23600	7200	−7200	3600	−720

(3); then, we get the following system of nonlinear ordinary differential equations:

$$\begin{aligned}&\vartheta^\circ_{\ell+2}+57\vartheta^\circ_{\ell+1}+302\vartheta^\circ_{\ell}+302\vartheta^\circ_{\ell-1}+57\vartheta^\circ_{\ell-2}+\vartheta^\circ_{\ell-3}\\&\quad+\frac{6d}{\hbar}\left(\vartheta_{\ell+2}+25\vartheta_{\ell+1}+40\vartheta_{\ell}-40\vartheta_{\ell-1}-25\vartheta_{\ell-2}-\vartheta_{\ell-3}\right)\\&\quad-\frac{30\mu}{\hbar^2}\left(\vartheta^\circ_{\ell+2}+9\vartheta^\circ_{\ell+1}-10\vartheta^\circ_{\ell}-10\vartheta^\circ_{\ell-1}+9\vartheta^\circ_{\ell-2}+\vartheta^\circ_{\ell-3}\right)=0,\end{aligned} \tag{10}$$

where $d=1+\zeta z_\ell=1+\zeta(\vartheta_{\ell-3}+57\vartheta_{\ell-2}+302\vartheta_{\ell-1}+302\vartheta_{\ell}+57\vartheta_{\ell+1}+\vartheta_{\ell+2})^p$ and $^\circ$ denote derivative with respect to time.

The unknown parameters ϑ_ℓ and ϑ°_ℓ are linearly interpolated between n and $n+1$ (n and $n+1$ are two time levels) via the the Crank-Nicolson formula and the usual forward difference formula, respectively, as follows:

$$\vartheta_\ell=\frac{\vartheta_\ell^{n+1}+\vartheta_\ell^{n}}{2},\ \vartheta^\circ_\ell=\frac{\vartheta_\ell^{n+1}-\vartheta_\ell^{n}}{\Delta\tau}, \tag{11}$$

where ϑ_ℓ^n denotes the parameters at time $n\Delta\tau$. Then, by making use of equation (11), it follows that

$$\begin{aligned}&\alpha_{\ell1}\vartheta^{n+1}_{\ell-3}+\alpha_{\ell2}\vartheta^{n+1}_{\ell-2}+\alpha_{\ell3}\vartheta^{n+1}_{\ell-1}+\alpha_{\ell4}\vartheta^{n+1}_{\ell}+\alpha_{\ell5}\vartheta^{n+1}_{\ell+1}+\alpha_{\ell6}\vartheta^{n+1}_{\ell+2}\\&\quad=\alpha_{\ell6}\vartheta^{n}_{\ell-3}+\alpha_{\ell5}\vartheta^{n}_{\ell-2}+\alpha_{\ell4}\vartheta^{n}_{\ell-1}+\alpha_{\ell3}\vartheta^{n}_{\ell}+\alpha_{\ell2}\vartheta^{n}_{\ell+1}+\alpha_{\ell1}\vartheta^{n}_{\ell+2},\end{aligned} \tag{12}$$

where

$$\begin{aligned}\alpha_{\ell1}&=\hbar^2-3\hbar d\Delta\tau-30\mu,\\\alpha_{\ell2}&=57\hbar^2-75\hbar d\Delta\tau-270\mu,\\\alpha_{\ell3}&=302\hbar^2-120\hbar d\Delta\tau+300\mu,\\\alpha_{\ell4}&=302\hbar^2+120\hbar d\Delta\tau+300\mu,\\\alpha_{\ell5}&=57\hbar^2+75\hbar d\Delta\tau-270\mu,\\\alpha_{\ell6}&=\hbar^2+3\hbar d\Delta\tau-30\mu.\end{aligned} \tag{13}$$

The system (12) consisting of the $(\mathrm{J}+1)$ equations with $(\mathrm{J}+6)$ unknown parameters. It can be solved uniquely if we eliminate the parameters $\vartheta^{n+1}_{-3}, \vartheta^{n+1}_{-2}, \vartheta^{n+1}_{-1}, \vartheta^{n+1}_{\mathrm{J}+1}, \vartheta^{n+1}_{\mathrm{J}+2}$ by using the five *B.Cs* $\sigma(\rho_1,\tau)=\beta_1, \sigma(\rho_2,\tau)=\beta_2, \sigma_\eta(\rho_1,\tau)=\sigma_\eta(\rho_2,\tau)=\sigma_{\eta\eta}(\rho_1,\tau)=0$; that is,

$$\begin{aligned}&\vartheta^{n+1}_{-3}+57\vartheta^{n+1}_{-2}+302\vartheta^{n+1}_{-1}+302\vartheta^{n+1}_{0}+57\vartheta^{n+1}_{1}+\vartheta^{n+1}_{2}=\beta_1,\\&\frac{6}{\hbar}\left(\vartheta^{n+1}_{2}+25\vartheta^{n+1}_{1}+40\vartheta^{n+1}_{0}-40\vartheta^{n+1}_{-1}-25\vartheta^{n+1}_{-2}-\vartheta^{n+1}_{-3}\right)=0,\\&\frac{30}{\hbar^2}\left(\vartheta^{n+1}_{2}+9\vartheta^{n+1}_{1}-10\vartheta^{n+1}_{0}-10\vartheta^{n+1}_{-1}+9\vartheta^{n+1}_{-2}+\vartheta^{n+1}_{-3}\right)=0,\\&\vartheta^{n+1}_{\mathrm{J}-3}+57\vartheta^{n+1}_{\mathrm{J}-2}+302\vartheta^{n+1}_{\mathrm{J}-1}+302\vartheta^{n+1}_{\mathrm{J}}+57\vartheta^{n+1}_{\mathrm{J}+1}+\vartheta^{n+1}_{\mathrm{J}+2}=\beta_2,\\&\frac{6}{\hbar}\left(\vartheta^{n+1}_{\mathrm{J}+2}+25\vartheta^{n+1}_{\mathrm{J}+1}+40\vartheta^{n+1}_{\mathrm{J}+1}-40\vartheta^{n+1}_{\mathrm{J}-1}-25\vartheta^{n+1}_{\mathrm{J}-2}-\vartheta^{n+1}_{\mathrm{J}-3}\right)=0.\end{aligned} \tag{14}$$

Consequently, we get a matrix system of dimension $(\mathrm{J}+1)\times(\mathrm{J}+1)$, and one can solve it easily by using a variant of the Thomas algorithm.

To deal with nonlinearity in (12) at each time step, we carry out the following corrector methods:

(1) Approximating ϑ^{n+1} by using the following simple corrector:

$$(\vartheta^*)^{n+1}=\vartheta^n+\frac{\vartheta^{n+1}-\vartheta^n}{2} \tag{15}$$

(2) As an approximation for ϑ^{n+1}, we use $(\vartheta^*)^{n+1}$

(3) Repeating this procedure twice at time step $n+1$ to refine ϑ^{n+1}

(4) Repeating this procedure at each time step along the execution of the program

The iterative procedure ϑ_ℓ^n in (4) can start by determining the initial parameters ϑ_ℓ^0, and it can be determined by making use of the *B.Cs* (4), *I.C.* (5), and the following requirements:

$$\begin{aligned}\sigma'_{\mathrm{J}}(\rho_1,0)&=\vartheta^0_2+25\vartheta^0_1+40\vartheta^0_0-40\vartheta^0_{-1}-25\vartheta^0_{-2}-\vartheta^0_{-3}=0,\\\sigma''_{\mathrm{J}}(\rho_1,0)&=\vartheta^0_2+9\vartheta^0_1-10\vartheta^0_0-10\vartheta^0_{-1}+9\vartheta^0_{-2}+\vartheta^0_{-3}=0,\\\sigma^{(3)}_{\mathrm{J}}(\rho_1,0)&=\vartheta^0_{\ell+2}+\vartheta^0_{\ell+1}-8\vartheta^0_{\ell}+8\vartheta^0_{\ell-1}-\vartheta^0_{\ell-2}-\vartheta^0_{\ell-3}=0,\\\sigma_{\mathrm{J}}(\eta_i,0)&=\vartheta^0_{j-3}+57\vartheta^0_{j-2}+302\vartheta^0_{j-1}+302\vartheta^0_{j}+57\vartheta^0_{j+1}+\vartheta^0_{j+2}\\&=f\left(\eta_j\right),\quad j=0,1,\cdots,\mathrm{J},\\\sigma'_{\mathrm{J}}(\rho_1,0)&=\vartheta^0_{\mathrm{J}+2}+25\vartheta^0_{\mathrm{J}+1}+40\vartheta^0_{\mathrm{J}+1}-40\vartheta^0_{\mathrm{J}-1}-25\vartheta^0_{\mathrm{J}-2}-\vartheta^0_{\mathrm{J}-3}=0,\\\sigma''_{\mathrm{J}}(\rho_1,0)&=\vartheta^0_{\mathrm{J}+2}+9\vartheta^0_{\mathrm{J}+1}-10\vartheta^0_{\mathrm{J}}-10\vartheta^0_{\mathrm{J}-1}+9\vartheta^0_{\mathrm{J}-2}+\vartheta^0_{\mathrm{J}-3}=0.\end{aligned} \tag{16}$$

Again, one can solve it by a variant of the Thomas algorithm and the approximate solution $\sigma^{(i)}_{\mathrm{J}}(\eta,\tau), i=0,1,\cdots,5$ that can be obtained from equation (9).

Now, we can apply the von Neumann stability method to establish the stability of the scheme (12), but the von Neumann stability method is applicable to linear schemes; so, we shall line arise the nonlinear term $\sigma^p\sigma_\eta$ by taking σ as a constant value k, and thus the nonlinear term becomes $\sigma^p = z_\ell = k^p$. Then, by substitution the Fourier mode $\vartheta_\ell^n = \hat{p}^n e^{i\ell\varphi}$ into our linearized form of equation (12) with writing $\hat{p}^{n+1} = q\hat{p}^n$, we get

$$q = \frac{\mathscr{A}_1 + i\mathscr{A}_2}{\mathscr{A}_3 + i\mathscr{A}_4}, \tag{17}$$

where q is growth factor and

$$\begin{aligned}
\mathscr{A}_1 &= \alpha_{\ell 6}\cos(3\varphi) + (\alpha_{\ell 5} + \alpha_{\ell 1})\cos(2\varphi) + (\alpha_{\ell 4} + \alpha_{\ell 2})\cos(\varphi) + \alpha_{\ell 3},\\
\mathscr{A}_2 &= -\alpha_{\ell 6}\sin(3\varphi) - (\alpha_{\ell 5} - \alpha_{\ell 1})\sin(2\varphi) - (\alpha_{\ell 4} - \alpha_{\ell 2})\sin(\varphi),\\
\mathscr{A}_3 &= \alpha_{\ell 1}\cos(3\varphi) + (\alpha_{\ell 2} + \alpha_{\ell 6})\cos(2\varphi) + (\alpha_{\ell 3} + \alpha_{\ell 5})\cos(\varphi) + \alpha_{\ell 4},\\
\mathscr{A}_4 &= -\alpha_{\ell 1}\sin(3\varphi) - (\alpha_{\ell 2} - \alpha_{\ell 6})\sin(2\varphi) - (\alpha_{\ell 3} - \alpha_{\ell 2})\sin(\varphi).
\end{aligned} \tag{18}$$

Thanks to Python software, we obtain same expressions for $\mathscr{A}_1^2 + \mathscr{A}_2^2$ and $\mathscr{A}_3^2 + \mathscr{A}_4^2$ in the following form:

$$\begin{aligned}
\mathscr{A}_1^2 + \mathscr{A}_2^2 = \mathscr{A}_3^2 + \mathscr{A}_4^2 = \big[&\sin(\varphi)\left(-\left(245\hbar^2 + 195\hbar d\Delta\tau + 570\mu\right)\right)\\
&- \sin(2\varphi)\left(56\hbar^2 + 78\hbar d\Delta\tau - 240\mu\right)\\
&+ \sin(3\varphi)\left(-\hbar^2 - 3\hbar d\Delta\tau + 30\mu\right)\big]^2\\
&+ \big[\cos(\varphi)\left(359\hbar^2 + 45\hbar d\Delta\tau + 30\mu\right)\\
&+ \cos(2\varphi)\left(58\hbar^2 + 72\hbar d\Delta\tau - 300\mu\right)\\
&+ \cos(3\varphi)\left(\hbar^2 + 3\hbar d\Delta\tau - 30\mu\right)\\
&+ 302\hbar^2 - 120\hbar d\Delta\tau + 300\mu\big]^2,
\end{aligned} \tag{19}$$

in order for the magnitude of the growth factor that is$|q| = 1$, and thus the linearized numerical algorithm for the GMRLW equation will be unconditionally stable.

2.2. The SBCM2. One can split equation (3) as a system of partial differential equation:

$$\left(\sigma - \mu\sigma_{\eta\eta}\right)_\tau + 2\zeta\sigma^p\sigma_\eta = 0, \tag{20}$$

$$\left(\sigma - \mu\sigma_{\eta\eta}\right)_\tau + 2\sigma_\eta = 0. \tag{21}$$

To applied the collocation approach for system (20) and (21), we identify the collocation points with the nodes η_i, $i = 0, 1, \cdots, \mathrm{J}$. If we put the approximation (7) into equations (20) and (21), we can obtain the following system of 1st order ordinary differential equations:

$$\begin{aligned}
&\vartheta^\circ_{\ell+2} + 57\vartheta^\circ_{\ell+1} + 302\vartheta^\circ_\ell + 302\vartheta^\circ_{\ell-1} + 57\vartheta^\circ_{\ell-2} + \vartheta^\circ_{\ell-3}\\
&\quad - \frac{30\mu}{\hbar^2}\left(\vartheta^\circ_{\ell+2} + 9\vartheta^\circ_{\ell+1} - 10\vartheta^\circ_\ell - 10\vartheta^\circ_{\ell-1} + 9\vartheta^\circ_{\ell-2} + \vartheta^\circ_{\ell-3}\right)\\
&= 0 + \frac{12\zeta z_\ell}{\hbar}\left(\vartheta_{\ell+2} + 25\vartheta_{\ell+1} + 40\vartheta_\ell - 40\vartheta_{\ell-1} - 25\vartheta_{\ell-2} - \vartheta_{\ell-3}\right),
\end{aligned} \tag{22}$$

$$\begin{aligned}
&\vartheta^\circ_{\ell+2} + 57\vartheta^\circ_{\ell+1} + 302\vartheta^\circ_\ell + 302\vartheta^\circ_{\ell-1} + 57\vartheta^\circ_{\ell-2} + \vartheta^\circ_{\ell-3}\\
&\quad - \frac{30\mu}{\hbar^2}\left(\vartheta^\circ_{\ell+2} + 9\vartheta^\circ_{\ell+1} - 10\vartheta^\circ_\ell - 10\vartheta^\circ_{\ell-1} + 9\vartheta^\circ_{\ell-2} + \vartheta^\circ_{\ell-3}\right)\\
&= 0 + \frac{12}{\hbar}\left(\vartheta_{\ell+2} + 25\vartheta_{\ell+1} + 40\vartheta_\ell - 40\vartheta_{\ell-1} - 25\vartheta_{\ell-2} - \vartheta_{\ell-3}\right),
\end{aligned} \tag{23}$$

where $^\circ$ is defined in (10), and nonlinearity term is $z_\ell = (\vartheta_{\ell-3} + 57\vartheta_{\ell-2} + 302\vartheta_{\ell-1} + 302\vartheta_\ell + 57\vartheta_{\ell+1} + \vartheta_{\ell+2})^p$. Approximating the parameters ϑ_ℓ between n and $n+1/2$ by using the Crank-Nicolson formula and ϑ°_ℓ by using the finite difference rule as follows:

$$\vartheta_\ell = \frac{\vartheta_\ell^{n+1/2} + \vartheta_\ell^n}{4}, \vartheta^\circ_\ell = \frac{\vartheta_\ell^{n+1/2} - \vartheta_\ell^n}{\Delta\tau}. \tag{24}$$

Thus, equation (22) becomes

$$\begin{aligned}
&\alpha_1\vartheta_{\ell-3}^{n+1/2} + \alpha_2\vartheta_{\ell-2}^{n+1/2} + \alpha_3\vartheta_{\ell-1}^{n+1/2} + \alpha_4\vartheta_\ell^{n+1/2} + \alpha_5\vartheta_{\ell+1}^{n+1/2} + \alpha_6\vartheta_{\ell+2}^{n+1/2}\\
&\quad = \alpha_6\vartheta_{\ell-3}^n + \alpha_5\vartheta_{\ell-2}^n + \alpha_4\vartheta_{\ell-1}^n + \alpha_3\vartheta_\ell^n + \alpha_2\vartheta_{\ell+1}^n + \alpha_1\vartheta_{\ell+2}^n,
\end{aligned} \tag{25}$$

where

$$\begin{aligned}
\alpha_1 &= \hbar^2 - 3\hbar\zeta z_\ell\Delta\tau - 30\mu,\\
\alpha_2 &= 57\hbar^2 - 75\hbar\zeta z_\ell\Delta\tau - 270\mu,\\
\alpha_3 &= 302\hbar^2 - 120\hbar\zeta z_\ell\Delta\tau + 300\mu,\\
\alpha_4 &= 302\hbar^2 + 120\hbar\zeta z_\ell\Delta\tau + 300\mu,\\
\alpha_5 &= 57\hbar^2 + 75\hbar\zeta z_\ell\Delta\tau - 270\mu,\\
\alpha_6 &= \hbar^2 + 3\hbar\zeta z_\ell\Delta\tau - 30\mu.
\end{aligned} \tag{26}$$

Analogously, in view of the Crank-Nicolson and forward finite difference approaches in time, both parameters ϑ_ℓ and ϑ°_ℓ are linearly interpolated between two time levels $n+1/2$ and $n+1$, respectively, as follows:

$$\vartheta_\ell = \frac{\vartheta_\ell^{n+1} + \vartheta_\ell^{n+1/2}}{4}, \quad \vartheta^\circ_\ell = \frac{\vartheta_\ell^{n+1} - \vartheta_\ell^{n+1/2}}{\Delta\tau}. \tag{27}$$

Thus, equation (23) becomes

$$\begin{aligned}&\alpha_7\vartheta_{\ell-3}^{n+1}+\alpha_8\vartheta_{\ell-2}^{n+1}+\alpha_9\vartheta_{\ell-1}^{n+1}+\alpha_{10}\vartheta_{\ell}^{n+1}+\alpha_{11}\vartheta_{\ell+1}^{n+1}+\alpha_{12}\vartheta_{\ell+2}^{n+1}\\&\quad=\alpha_{12}\vartheta_{\ell-3}^{n+1/2}+\alpha_{11}\vartheta_{\ell-2}^{n+1/2}+\alpha_{10}\vartheta_{\ell-1}^{n+1/2}+\alpha_9\vartheta_{\ell}^{n+1/2}\\&\qquad+\alpha_8\vartheta_{\ell+1}^{n+1/2}+\alpha_7\vartheta_{\ell+2}^{n+1/2},\end{aligned}\tag{28}$$

where

$$\begin{aligned}\alpha_7&=\hbar^2-30\mu-3\hbar\Delta\tau,\\\alpha_8&=57\hbar^2-75\hbar\Delta\tau-270\mu,\\\alpha_9&=302\hbar^2+300\mu-120\hbar\Delta\tau,\\\alpha_{10}&=302\hbar^2+120\hbar\Delta\tau+300\mu,\\\alpha_{11}&=57\hbar^2-270\mu+75\hbar\Delta\tau,\\\alpha_{12}&=\hbar^2+3\hbar\Delta\tau-30\mu.\end{aligned}\tag{29}$$

Equations (25) and (28) constitute the numerical algorithms for the GMRLW equation. We can remove the nonlinearity terms occurring in equation (25) by replacing ϑ_ℓ by ϑ_ℓ^n in z_ℓ, and thus the equation (25) will be linearized.

Therefore, we see that the iterative systems of equations (25) and (28) consist the $(\mathrm{J}+1)$ equations in the $(\mathrm{J}+6)$ unknown parameters, and one can solve it by eliminating the parameters $\vartheta_{-3}^j, \vartheta_{-2}^j, \vartheta_{-1}^j, \vartheta_{\mathrm{J}+1}^j, \vartheta_{\mathrm{J}+2}^j$, $j=n+1/2, n+1$ by making use of the five *B.Cs* $\sigma(\rho_1,\tau)=\beta_1, \sigma(\rho_2,\tau)=\beta_2, \sigma_\eta(\rho_1,\tau)=\sigma_\eta(\rho_2,\tau)=\sigma_{\eta\eta}(\rho_1,\tau)=0$; then, we can obtain

$$\begin{aligned}&\vartheta_{-3}^j+57\vartheta_{-2}^j+302\vartheta_{-1}^j+302\vartheta_0^j+57\vartheta_1^j+\vartheta_2^j=\beta_1,\\&\frac{6}{\hbar}\left(\vartheta_2^j+25\vartheta_1^j+40\vartheta_0^j-40\vartheta_{-1}^j-25\vartheta_{-2}^j-\vartheta_{-3}^j\right)=0,\\&\frac{30}{\hbar^2}\left(\vartheta_2^j+9\vartheta_1^j-10\vartheta_0^j-10\vartheta_{-1}^j+9\vartheta_{-2}^j+\vartheta_{-3}^j\right)=0,\\&\vartheta_{\mathrm{J}-3}^j+57\vartheta_{\mathrm{J}-2}^j+302\vartheta_{\mathrm{J}-1}^j+302\vartheta_{\mathrm{J}}^j+57\vartheta_{\mathrm{J}+1}^j+\vartheta_{\mathrm{J}+2}^j=\beta_2,\\&\frac{6}{\hbar}\left(\vartheta_{\mathrm{J}+2}^j+25\vartheta_{\mathrm{J}+1}^j+40\vartheta_{\mathrm{J}+1}^j-40\vartheta_{\mathrm{J}-1}^j-25\vartheta_{\mathrm{J}-2}^j-\vartheta_{\mathrm{J}-3}^j\right)=0.\end{aligned}\tag{30}$$

Thus, we get a matrix system of dimension $(\mathrm{J}+1)\times(\mathrm{J}+1)$, and we can easily solve it by using a variant of the Thomas algorithm.

To deal with nonlinearity in (28) at each time step, we carry out the following corrector procedure:

$$(\vartheta^*)_i^j=\vartheta_i^n+\frac{\vartheta_i^j-\vartheta_i^n}{2}.\tag{31}$$

This iterative scheme is executed two times by determining $(\vartheta^*)_i^j$ for ϑ_i^j, where $j=n+1/2, n+1$.

We start the time evolution of the ϑ_ℓ^j, $j=n+1/2, n+1$ using (25) and (28) by calculating initial parameters ϑ_ℓ^0. Therefore, the approximate solution (8) must agree with the *I.C.* at the knots, and this leads to $\mathrm{J}+1$ equations. Also, the further five equations can be obtained by using the derivatives of σ_J in (8) at the ends:

$$\begin{aligned}&\sigma'_\mathrm{J}(\rho_1,0)=\vartheta_2^0+25\vartheta_1^0+40\vartheta_0^0-40\vartheta_{-1}^0-25\vartheta_{-2}^0-\vartheta_{-3}^0=0,\\&\sigma''_\mathrm{J}(\rho_1,0)=\vartheta_2^0+9\vartheta_1^0-10\vartheta_0^0-10\vartheta_{-1}^0+9\vartheta_{-2}^0+\vartheta_{-3}^0=0,\\&\sigma_\mathrm{J}^{(3)}(\rho_1,0)=\vartheta_{\ell+2}^0+\vartheta_{\ell+1}^0-8\vartheta_\ell^0+8\vartheta_{\ell-1}^0-\vartheta_{\ell-2}^0-\vartheta_{\ell-3}^0=0,\\&\sigma_\mathrm{J}(\eta_i,0)=\vartheta_{j-3}^0+57\vartheta_{j-2}^0+302\vartheta_{j-1}^0+302\vartheta_j^0+57\vartheta_{j+1}^0+\vartheta_{j+2}^0\\&\qquad=f\left(\eta_j\right),\quad j=0,1,\cdots,\mathrm{J},\\&\sigma'_\mathrm{J}(\rho_1,0)=\vartheta_{\mathrm{J}+2}^0+25\vartheta_{\mathrm{J}+1}^0+40\vartheta_{\mathrm{J}+1}^0-40\vartheta_{\mathrm{J}-1}^0-25\vartheta_{\mathrm{J}-2}^0-\vartheta_{\mathrm{J}-3}^0=0,\\&\sigma''_\mathrm{J}(\rho_1,0)=\vartheta_{\mathrm{J}+2}^0+9\vartheta_{\mathrm{J}+1}^0-10\vartheta_{\mathrm{J}}^0-10\vartheta_{\mathrm{J}-1}^0+9\vartheta_{\mathrm{J}-2}^0+\vartheta_{\mathrm{J}-3}^0=0.\end{aligned}\tag{32}$$

Consequently, the parameters $\vartheta_i^0, i=-3,-2,\cdots,\mathrm{J}+2$ will be determined as solution of a matrix equation.

To establish the stability of the scheme (25), we carry out the von Neumann stability scheme by linearizing the nonlinear term $\sigma^p\sigma_\eta$ by taking σ as a constant k so that σ^p becomes $\sigma^p=z_\ell=k^p$. By substitution the Fourier mode of $\vartheta_\ell^n=\hat{p}^n e^{i\ell\varphi}$ into our linearized form of equation (25) and by writing $\hat{p}^{n+1}=q\hat{p}^n$ in the resulting iterative equation, we can deduce

$$q=\frac{\mathscr{A}_1+i\mathscr{A}_2}{\mathscr{A}_3+i\mathscr{A}_4},\tag{33}$$

where

$$\begin{aligned}\mathscr{A}_1&=\alpha_3+(\alpha_1+\alpha_5)\cos(2\varphi)+(\alpha_2+\alpha_4)\cos(\varphi)+\alpha_6\cos(3\varphi),\\\mathscr{A}_2&=(\alpha_1-\alpha_5)\sin(2\varphi)+(\alpha_2-\alpha_4)\sin(\varphi)-\alpha_6\sin(3\varphi),\\\mathscr{A}_3&=\alpha_4+(\alpha_2+\alpha_6)\cos(2\varphi)+\alpha_1\cos(3\varphi)+(\alpha_3+\alpha_5)\cos(\varphi),\\\mathscr{A}_4&=(\alpha_2-\alpha_3)\sin(\varphi)+(\alpha_6-\alpha_2)\sin(2\varphi)-\alpha_1\sin(3\varphi).\end{aligned}\tag{34}$$

Here, note that the von Neumann condition is fulfilled; that is, $|q|\le 1$. This affects the difference scheme (25) to be unconditionally stable. In the same way, we can show that the difference equation (28) can be unconditionally stable as well.

3. Numerical Calculations

Here, numerical tests are presented to demonstrate the performance of our proposed algorithm for single and

Table 2: Error norms and invariants for the single solitary wave for the above parameters.

Time	Method	$\mathscr{L}_2 \times 10^4$	$\mathscr{L}_\infty \times 10^4$	χ_1	χ_2	χ_3
	Analytical			7.809875	2.129887	0.130250
0	SBCM1	0.0	0.0	7.809702	2.129886	0.130251
	SBCM2	0.0	0.0	7.809702	2.129886	0.130251
1	SBCM1	0.000899	0.000497	7.809725	2.129887	0.130251
	SBCM2	0.001982	0.001588	7.809725	2.129887	0.130251
2	SBCM1	0.000481	0.000681	7.809744	2.129887	0.130250
	SBCM2	0.000986	0.000966	7.809744	2.129887	0.130250
3	SBCM1	0.000979	0.000381	7.809767	2.129887	0.130250
	SBCM2	0.001081	0.002124	7.809767	2.129887	0.130250
4	SBCM1	0.002519	0.000994	7.809783	2.129887	0.130250
	SBCM2	0.006957	0.004066	7.809783	2.129887	0.130250
5	SBCM1	0.007738	0.005744	7.809800	2.129887	0.130250
	SBCM2	0.009886	0.008759	7.809800	2.129887	0.130250
6	SBCM1	0.009956	0.008964	7.809819	2.129887	0.130250
	SBCM2	0.011042	0.012464	7.809819	2.129887	0.130250
7	SBCM1	0.010009	0.009979	7.809841	2.129887	0.130250
	SBCM2	0.021244	0.010012	7.809841	2.129887	0.130250
8	SBCM1	0.013692	0.010210	7.809855	2.129887	0.130250
	SBCM2	0.033897	0.021252	7.809855	2.129887	0.130250
9	SBCM1	0.024350	0.013776	7.809868	2.129887	0.130250
	SBCM2	0.039873	0.028806	7.809868	2.129887	0.130250
10	SBCM1	0.026879	0.010968	7.809874	2.129887	0.130251
	SBCM2	0.035471	0.026398	7.809874	2.129887	0.130251
10	[20]	6.982800	1.995240	7.809320	2.129880	0.130315
10	[23]	0.048674	0.033611	7.807948	2.129887	0.130251

interactions of multiple solitary waves. Also, the modified Maxwellian *I.C.*s are pointed out to generate a train of solitary waves. Furthermore, the accuracy of the presented schemes is measured in terms of the following discrete error norms $\mathscr{L}_2$ and $\mathscr{L}_\infty$:

$$\mathscr{L}_2 = \sqrt{\hbar \sum_{i=0}^{\mathrm{J}} \left|\sigma_i^{\mathrm{exact}} - \left(\sigma_{\mathrm{J}}\right)_i\right|^2}, \quad \mathscr{L}_\infty = \left\|\sigma^{\mathrm{exact}} - \sigma_{\mathrm{J}}\right\|_\infty = \max_i \left|\sigma_i^{\mathrm{exact}} - \left(\sigma_{\mathrm{J}}\right)_i\right|. \tag{35}$$

The conservation properties of the MRLW equation related to energy, mass, and momentum can be determined by finding the three basic invariants [24, 25]:

$$\chi_1 = \int_{\rho_1}^{\rho_2} \sigma dx, \quad \chi_2 = \int_{\rho_1}^{\rho_2} \left[\sigma^2 + \mu\left(\sigma_\eta\right)^2\right] dx, \quad \chi_3 = \int_{\rho_1}^{\rho_2} \left[\sigma^4 - \frac{6}{\zeta}\mu\left(\sigma_\eta\right)^2\right] dx. \tag{36}$$

3.1. Single Solitary Wave. Let η_0 be any arbitrary constant. Then, the exact solution of the solitary wave of the MRLW equation is given as follows [20]:

$$\sigma(\eta, \tau) = \sqrt{\frac{6\lambda}{\zeta}} \operatorname{sech}\left(\sqrt{\frac{\lambda}{\mu(\lambda+1)}}\left(\eta - (\lambda+1)\tau - \eta_0\right)\right). \tag{37}$$

The modified Maxwellian *I.C.* is defined by

$$\sigma(\eta, 0) = \sqrt{\frac{6\lambda}{\zeta}} \operatorname{sech}\left(\sqrt{\frac{\lambda}{\mu(\lambda+1)}}\left(\eta - \eta_0\right)\right), \tag{38}$$

and the *B.C*s can be concluded from the exact equation.

We choose $\zeta = \mu = 1, \lambda = 0.1, \hbar = 0.125, \Delta\tau = 0.1, \eta_0 = 0$, $-40 \le \eta \le 60$ so that we can compare our results with results in [20, 23]. The program is executed up to times $\tau = 10$ to find error norms and the invariants χ_1, χ_2, χ_3 at different times, and the results are given in Table 2. From Table 2, one can observe that the predicted error norms $\mathscr{L}_2$ and $\mathscr{L}_\infty$ are smaller than those obtained in [20, 23], and also the invariants χ_1, χ_2, and χ_3 are sanely in good agreement with their

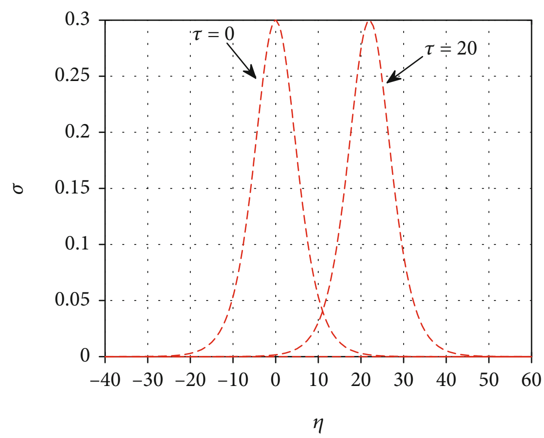

Figure 1: Plot illustration for a single solitary wave solution at $\tau = 0$ and 20.

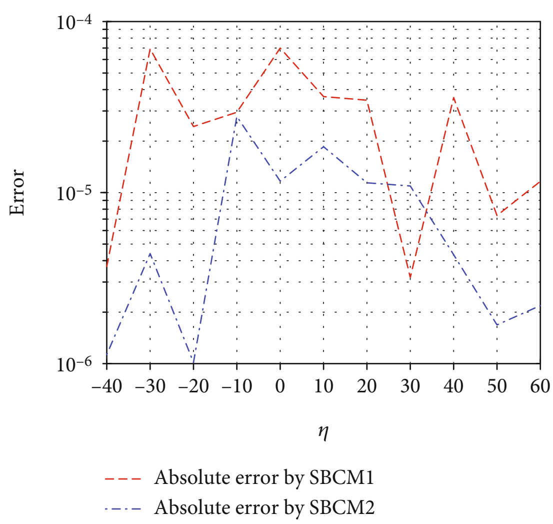

Figure 2: Absolute error distribution at $\tau = 10$ for SBCM1 and SBCM2.

exact values. The solutions at $\tau = 0, 20$ and the motion of the solitary wave along with the interval $-40 \leq \eta \leq 60$ with $0 \leq \tau \leq 20$ to the right are illustrated in Figure 1. Moreover, the error variations are demonstrated for the proposed algorithms SBCM1 and SBCM2 in Figure 2 at time $\tau = 10$. Consequently, we can observe from Table 2 that the results obtained by the SBCM2 are more accurate than those obtained by the SBCM1.

3.2. Two Solitary Waves. Now, we study the interaction of two solitary waves having different amplitudes, which is the sum of two modified Maxwellian *I.C.*:

$$\sigma(\eta, 0) = \sum_{j=1}^{2} \sqrt{\frac{6\lambda_j}{\zeta}} \operatorname{sech} \left(\sqrt{\frac{\lambda_j}{\mu(\lambda_j + 1)}} (\eta - \eta_j) \right). \quad (39)$$

Here, we take the parameters $\zeta = 6, \lambda_1 = 4, \lambda_2 = 1, \eta_1 = 25, \eta_2 = 55, \hbar = 0.2, \Delta\tau = 0.025, \mu = 1, \eta_0 = 0, 0 \leq \eta \leq 200$ to

Table 3: Two solitary waves invariants for the above parameters.

Time	Method	χ_1	χ_2	χ_3
	Analytical	11.467698	14.629243	22.880466
0	SBCM1	11.467698	14.629258	22.880465
	SBCM2	11.467698	14.629260	22.880477
2	SBCM1	11.467698	14.629616	22.882143
	SBCM2	11.467698	14.628777	22.883803
4	SBCM1	11.467698	14.629946	22.886081
	SBCM2	11.467698	14.627551	22.888679
6	SBCM1	11.467698	14.629841	22.886133
	SBCM2	11.467699	14.627773	22.889057
8	SBCM1	11.467698	14.629800	22.889777
	SBCM2	11.467699	14.628916	22.873736
10	SBCM1	11.467699	14.629215	22.881137
	SBCM2	11.467699	14.628168	22.883663
12	SBCM1	11.467699	14.629275	22.885653
	SBCM2	11.467699	14.628557	22.871531
14	SBCM1	11.467699	14.629067	22.885269
	SBCM2	11.467700	14.628562	22.888816
16	SBCM1	11.467699	14.629554	22.885142
	SBCM2	11.467700	14.626609	22.874989
18	SBCM1	11.467699	14.629903	22.886686
	SBCM2	11.467700	14.629421	22.877228
20	SBCM1	11.467700	14.629287	22.885799
	SBCM2	11.467701	14.629190	22.874809
20	[22]	11.4677	14.6292	22.8809
20	[23]	11.467701	14.583089	22.696510
20	[26]	11.4661	14.6249	22.8631

concur with those used in [22, 23, 26]. The program is executed up to time $\tau = 20$, and the values of invariants χ_1, χ_2, χ_3 are shown in Table 3 and compared with those obtained in [22, 23, 26] at time $\tau = 20$. On the other hand, Figure 3 illustrates the interaction of solitary waves at the times $\tau = 0$ and $\tau = 15$, respectively.

3.3. Three Solitary Waves. Here, we study the MRLW equation with the modified Maxwellian *I.C.* and different amplitudes:

$$\sigma(\eta, 0) = \sum_{j=1}^{3} \sqrt{\frac{6\lambda_j}{\zeta}} \operatorname{sech}_{10} \left(\sqrt{\frac{\lambda_j}{\mu(\lambda_j + 1)}} (\eta - \eta_j) \right). \quad (40)$$

Numerical experiments are executed for the parameters $\zeta = 6, y = 0.2, \mu = 1, \Delta\tau = 0.025, \lambda_1 = 0.03, \lambda_2 = 0.02, \lambda_3 = 0.01, \eta_1 = 18, \eta_2 = 48, \eta_3 = 88$ in the region $-40 \leq \eta \leq 180$ in order to see an interaction of three solitary waves takes place. The program is executed up to time $\tau = 45$. Table 4 compares our obtained values of the invariants of the three solitary waves by SBCM2 with those obtained by [23]. It is clear from the table that our obtained results of the invariants remain

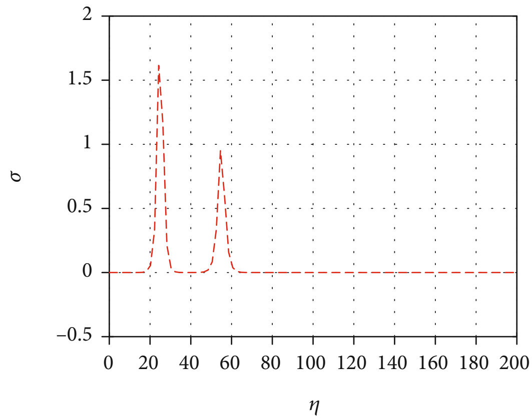

(a) $\tau = 0$

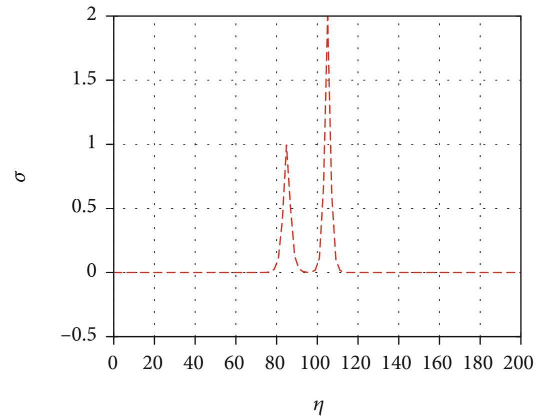

(b) $\tau = 15$

FIGURE 3: Plot illustrations for interaction of 2 solitary waves at $\tau = 0$ and $\tau = 15$.

TABLE 4: Invariants for 3 solitary waves for $\zeta = 6, \mu = 1, \hbar = 0.2, \Delta\tau = 0.025, \lambda_1 = 0.03, \lambda_2 = 0.02, \lambda_3 = 0.01, \eta_1 = 18, \eta_2 = 48, \eta_3 = 88, -40 \le \eta \le 180$.

Time	Our SBCM2			[23]		
	χ_1	χ_2	χ_3	χ_1	χ_2	χ_3
0.0	9.518251	0.904130	0.00786304	9.517705	0.904129	0.00786304
0.1	9.518016	0.904130	0.00786312	9.517580	0.904130	0.00786272
0.2	9.518193	0.904130	0.00786323	9.517585	0.904130	0.00786286
0.3	9.518101	0.904130	0.00786338	9.517590	0.904130	0.00786293
0.4	9.518130	0.904130	0.00786350	9.517594	0.904130	0.00786294
0.5	9.518145	0.904130	0.00786365	9.517598	0.904130	0.00786296
0.6	9.518159	0.904130	0.00786388	9.517602	0.904130	0.00786297
0.7	9.518177	0.904130	0.00786300	9.517606	0.904130	0.00786298
0.8	9.518185	0.904130	0.00786300	9.517610	0.904130	0.00786299
0.9	9.518197	0.904130	0.00786300	9.517613	0.904130	0.00786300
1.0	9.518253	0.904130	0.00786301	9.517616	0.904130	0.00786300

TABLE 5: Invariants for 3 solitary waves for $\mu = 1, \hbar = 0.2, \Delta\tau = 0.025, \lambda_1 = 4, \lambda_2 = 1, \lambda_3 = 0.25, \eta_1 = 15, \eta_2 = 45, \eta_3 = 60, 0 \le \eta \le 250$.

Time	Our SBCM1			[26]		
	χ_1	χ_2	χ_3	χ_1	χ_2	χ_3
0	14.980105	15.821789	22.992100	14.9801	15.8375	23.0081
5	14.988882	15.829547	22.914553	14.9799	15.8365	23.0036
10	14.986782	15.826933	22.935095	14.9850	15.8453	23.0207
15	14.986213	15.826005	22.940089	14.9809	15.8367	22.9986
20	14.984805	15.825383	22.954986	14.9790	15.8340	22.9927
25	14.983907	15.824426	22.962205	14.9780	15.8323	22.9876
30	14.983243	15.823337	22.977218	14.9777	15.8311	22.9827
35	14.981637	15.822498	22.999045	14.9778	15.8299	22.9779
40	14.980144	15.821066	22.997974	14.9795	15.8291	22.9728
45	14.980008	15.821781	22.996855	14.9534	15.8290	22.9649

almost the same during the computer run, and they are found to be very close to the results given in [23]. In addition, these are all in good agreement with their analytical results.

Also, numerical experiments are carried out for the parameters $\hbar = 0.2, \mu = 1, k = 0.025, \lambda_1 = 4, \lambda_2 = 1, \lambda_3 = 0.25, \eta_1 = 15, \eta_2 = 45, \eta_3 = 60, 0 \le \eta \le 250$. The computation is

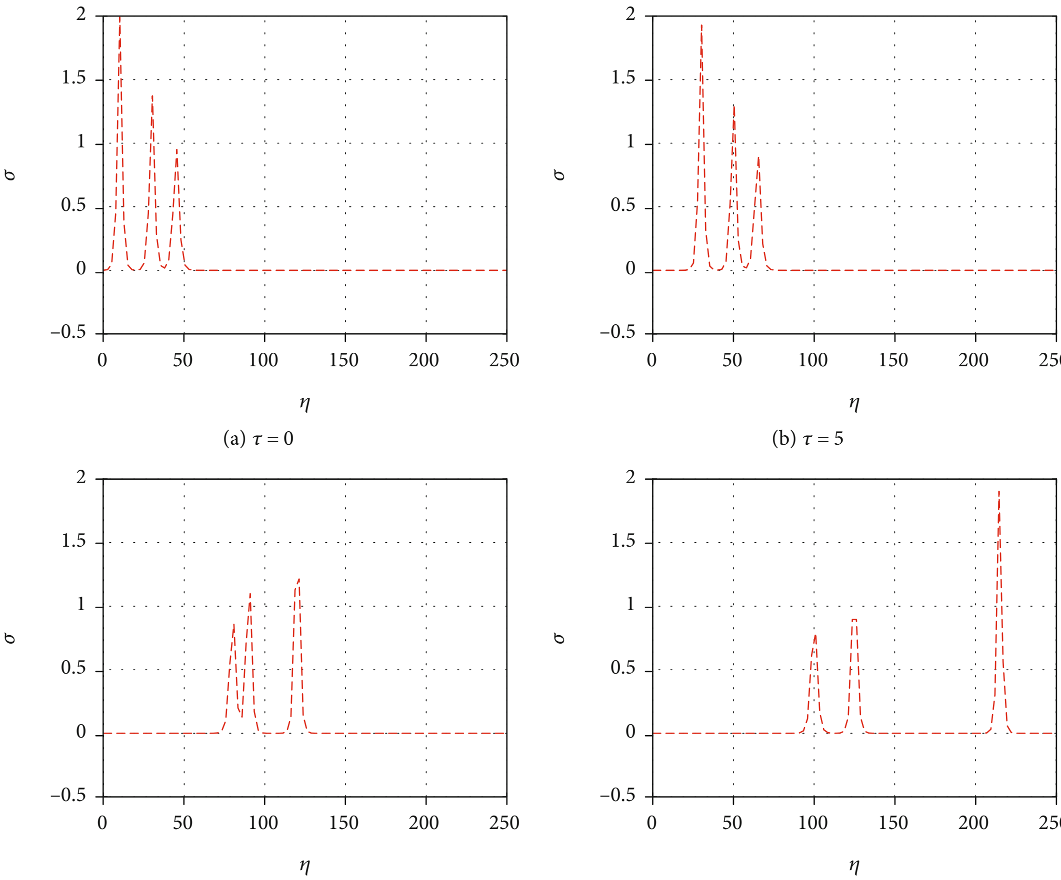

(a) $\tau = 0$ (b) $\tau = 5$ (c) $\tau = 20$ (d) $\tau = 35$

Figure 4: Plot illustrations for interaction of 3 solitary waves at $\tau = 5$, $\tau = 20$, and $\tau = 35$.

done until time $\tau = 45$ to find numerical results of the invariants χ_1, χ_2, χ_3. The result values of the invariants of the proposed SBCM2 algorithm together with the values of the invariants obtained in [26] are documented in Table 5.

In addition, we demonstrate the interaction of three solitary waves at times $\tau = 1, 5$ and $\tau = 10$, respectively, in Figure 4 and consequently, we can see that at time $\tau = 0, 5$, the three solitary waves interact and then at times $\tau = 20, 35$, the three solitary waves separate and emerging unchanged.

4. Conclusion

The main results of the article can be summarized as follows:

(i) The sextic B-spline collocation methods are presented to approximate a new solution of the MRLW equation

(ii) The unconditionally stability of the methods is derived

(iii) The operations are established by calculating both error norms $\mathscr{L}_2$ and $\mathscr{L}_\infty$

(iv) The numerical applications are demonstrated through examples of MRLW equations with the modified Maxwellian $I.C.$s

Data Availability

No data were used to support this study.

Conflicts of Interest

The authors declare that they have no conflicts interests.

Authors' Contributions

All authors contributed equally and significantly in writing this article. All authors read and approved the final manuscript.

Acknowledgments

This research was supported by the Taif University Researchers Supporting Project Number (TURSP-2020/217), Taif University, Taif, Saudi Arabia, and the Deanship of Scientific Research at Princess Nourah Bint Abdulrahman University through the Fast-Track Research Funding Program.

References

[1] D. H. Peregrine, "Calculations of the development of an undular bore," *Journal of Fluid Mechanics*, vol. 25, no. 2, pp. 321–330, 1966.

[2] T. B. Benjamin, J. L. Bona, and J. J. Mahony, "Model equations for waves in nonlinear dispersive system," *Philosophical Transactions. Royal Society of London*, vol. 227, pp. 47–78, 1972.

[3] J. L. Bona and P. J. Bryant, "A mathematical model for long waves generated by wavemakers in non-linear dispersive systems," *Proceedings of the Cambridge Philosophical Society*, vol. 73, no. 2, pp. 391–405, 1973.

[4] P. C. Jain, R. Shankar, and T. V. Singh, "Numerical solution of regularized long-wave equation," *Communications in Numerical Methods in Engineering*, vol. 9, no. 7, pp. 579–586, 1993.

[5] D. Bhardwaj and R. Shankar, "A computational method for regularized long wave equation," *Computers & Mathematcs with Applications*, vol. 40, no. 12, pp. 1397–1404, 2000.

[6] B.-Y. Guo and W.-M. Cao, "The fourier pseudospectral method with a restrain operator for the RLW equation," *Journal of Computational Physics*, vol. 74, no. 1, pp. 110–126, 1988.

[7] İ. Dağ and M. N. Özer, "Approximation of the RLW equation by the least square cubic B-spline finite element method," *Applied Mathematical Modelling*, vol. 25, no. 3, pp. 221–231, 2001.

[8] I. Dag, B. Saka, and D. Irk, "Application of cubic B-splines for numerical solution of the RLW equation," *Applied Mathematics and Computation*, vol. 159, no. 2, pp. 373–389, 2004.

[9] I. Dag, B. Saka, and D. Irk, "Galerkin method for the numerical solution of the RLW equation using quintic B-splines," *Journal of Computational and Applied Mathematics*, vol. 190, no. 1-2, pp. 532–547, 2006.

[10] S. U. Islam, S. Haq, and A. Ali, "A meshfree method for the numerical solution of the RLW equation," *Journal of Computational and Applied Mathematics*, vol. 223, no. 2, pp. 997–1012, 2009.

[11] Y. Gao and L. Mei, "Galerkin finite element methods for two-dimensional RLW and SRLW equations," *Applicable Analysis*, vol. 97, no. 13, pp. 2288–2312, 2017.

[12] L. Mei, Y. Gao, and Z. Chen, "Numerical study using explicit multistep Galerkin finite element method for the MRLW equation," *Numerical Methods for Partial Differential Equations*, vol. 31, no. 6, pp. 1875–1889, 2015.

[13] Y. Gao and L. Mei, "Mixed Galerkin finite element methods for modified regularized long wave equation," *Applied Mathematics and Computation*, vol. 258, pp. 267–281, 2015.

[14] D. Kaya and S. M. El-Sayed, "An application of the decomposition method for the generalized KDV and RLW equations," *Chaos, Solitons & Fractals*, vol. 17, no. 5, pp. 869–877, 2003.

[15] D. Kaya, "A numerical simulation of solitary-wave solutions of the generalized regularized long-wave equation," *Applied Mathematics and Computation*, vol. 149, no. 3, pp. 833–841, 2004.

[16] L. Zhang, "A finite difference scheme for generalized regularized long-wave equation," *Applied Mathematics and Computation*, vol. 168, no. 2, pp. 962–972, 2005.

[17] A. H. A. Ali, A. A. Soliman, and K. R. Raslan, "Soliton solution for nonlinear partial differential equations by cosine- function method," *Physics Letters A*, vol. 368, no. 3-4, pp. 299–304, 2007.

[18] L. R. T. Gardner, G. A. Gardner, F. A. Ayub, and N. K. Amein, "Approximations of solitary waves of the MRLW equation by B-spline, finite element," *Arabian Journal for Science and Engineering*, vol. 22, pp. 183–193, 1997.

[19] P. M. Prenter, *Splines and Variational Methods*, Wiley, New York, NY, USA, 1975.

[20] A. K. Khalifa, K. R. Raslan, and H. M. Alzubaidi, "A finite difference scheme for the MRLW and solitary wave interactions," *Applied Mathematics and Computation*, vol. 189, no. 1, pp. 346–354, 2007.

[21] A. K. Khalifa, K. R. Raslan, and H. M. Alzubaidi, "Numerical study using ADM for the modified regularized long wave equation," *Applied Mathematical Modelling*, vol. 32, no. 12, pp. 2962–2972, 2008.

[22] A. K. Khalifa, K. R. Raslan, and H. M. Alzubaidi, "A collocation method with cubic B-splines for solving the MRLW equation," *Journal of Computational and Applied Mathematics*, vol. 212, no. 2, pp. 406–418, 2008.

[23] F. Haq, S. Islam, and I. A. Tirmizi, "A numerical technique for solution of the MRLW equation using quartic B-splines," *Applied Mathematical Modelling*, vol. 34, no. 12, pp. 4151–4160, 2010.

[24] A. P. Hooper and R. Grimshaw, "Nonlinear instability at the interface between two viscous fluids," *Physics of Fluids*, vol. 28, no. 1, pp. 37–45, 1985.

[25] S. Natesan and N. Ramanujam, "Improvement of numerical solution of selfadjoint singular perturbation problems by incorporation of asymptotic approximations," *Applied Mathematics and Computation*, vol. 98, no. 2-3, pp. 119–137, 1999.

[26] S. B. G. Karakoci, T. Geyikli, and A. Bashan, "A numerical solution of the modified regularized long wave (MRLW) equation using quartic B-splines," *TWMS Journal of Applied and Engineering Mathematics*, vol. 3, no. 2, pp. 231–244, 2013.